DEUTSCHES ELEKTRONEN-SYNCHROTRON **DESY**
DESY 89-052
May 1989

Finite Temperature Symmetry Restoration in the 4-dimensional Ising Model

P. Seuferling
Deutsches Elektronen-Synchrotron DESY

ISSN 0418-9833

NOTKESTRASSE 85 · 2 HAMBURG 52

To be sure that your preprints are promptly included in the
HIGH ENERGY PHYSICS INDEX ,
send them to the following address (if possible by air mail) :

DESY
Bibliothek
Notkestrasse 85
2 Hamburg 52
Germany

DESY 89-052
May 1989

ISSN 0418-9833

Finite Temperature Symmetry Restoration in the 4-dimensional Ising Model

Peter Seuferling

Deutsches Elektronen-Synchrotron DESY, D-2000 Hamburg

May 5, 1989

Abstract

A finite temperature Monte Carlo simulation of the four-dimensional Ising model is presented and applied to lattices up to $20^3 \times 5$. A cluster algorithm is used which is especially suitable for simulations near the critical point. From the numerical data a value for the symmetry restoration temperature T_{sr} is derived and compared with continuum and lattice renormalized perturbation theory. A good agreement between the numerical measurements and the perturbative analysis is found.

1 Introduction

The Ising model as the limit of a single component ϕ^4 theory at infinite bare self coupling λ is the simplest lattice regularized quantum field theory QFT with scalar fields and a spontaneously broken global symmetry. This single component theory has many general properties in common with the four-component Φ^4 theory, which is the central part of the Higgs sector of the electroweak standard theory. Effects of a small gauge coupling can be described within the framework of a weak coupling expansion [1].

Therefore, much analytical and numerical work has already been done in this field. Two works concerning the Ising model shall be emphasized, because they will be important for this paper:

Montvay et al. [2] used Monte Carlo simulations of the Ising model for studying effects of the finite lattice size on physical quantities and for testing the scaling behaviour of renormalized quantities and the validity of renormalized perturbation theory in the broken phase.

In their analytical work Lüscher and Weisz [3] used a hopping parameter expansion (high temperature expansion) as an initial condition for the integration of the Callan-Symanzik equations in the scaling region, where the renormalized coupling is small enough. The solution of the renormalization group equation (RGE) is then continued over the critical line into the phase with spontaneously broken symmetry delivering the values of various renormalized quantities.

According to perturbative analyses in the continuum [4] [5] the ϕ^4 model has a phase transition at finite temperature, but the result is plagued by IR divergences near the critical point because of vanishing masses. In order to improve the results various non-perturbative, analytical methods have been applied [7]. A common feature of all these theories are the omission of certain graphs in the expansion and, therefore, unpredictable errors. An example for the confusion is a possible absurd symmtry non-restoration in special $O(N)\times O(N)$ models [8].

In addition, most of the analytical derivations of a critical temperature rely on the non-convexity of the effective potential, and symmetry restoration is indicated by the disappearence of the double-well form. However, it is well-known that in the continuum the effective potential is convex. [9].

Because of these technical difficulties a non-perturbative study of the lattice-regularized theory by MC-simulations seems to be necessary. Recently there have been MC simulations of the ϕ^4 theory at finite temperature, on the one hand, considering symmetry restoration in two and three dimensions [10] and, on the other hand, treating the problem of non-triviality for high temperature [11].

Beside technical reasons there is an additional physical motivation. Symmetry restoration has an important physical aspect in the theory of an inflationary universe [12]. This theory can solve a lot of problems concerning cosmology and particle physics by treating matter not as an ideal gas, but in terms of quantum fields and investigating a transition from a hot symmetric phase to a asymmetric phase, which takes place by tunneling due to quantum fluctuations. The symmetry restoration temperature T_{sr} determines the moment, when an exponential increase of the world radius begins and it is very important whether particles are produced before or afterwards.

2 Basic definitions

The bare Langrangian of the single component ϕ^4 theory with euclidean metric in the broken phase is

$$-L = \frac{1}{2}(\partial_\mu\phi_0(x))(\partial^\mu\phi_0(x)) + \frac{1}{2}m_0^2\phi_0(x)^2 + \frac{1}{6}g_0v_0\phi_0(x)^3 + \frac{1}{24}g_0\phi_0(x)^4 \qquad (1)$$

with

$$v_0^2 = \frac{3m_0^2}{g_0} \qquad (2)$$

The zero index marks the bare, unrenormalized quantities. According to a standard convention [13] the action on the lattice is

$$S = \sum_x \left\{ -2\kappa_s \sum_{i=1}^{3} \Phi(x)\Phi(x+\hat{i}) - 2\kappa_t\Phi(x)\Phi(x+\hat{4}) + \Phi(x)^2 + \lambda\left(\Phi(x)^2-1\right)^2 \right\} \qquad (3)$$

$\hat{\mu}$ with $\mu = 1,...,4$ is the unit vector in the μ-direction. κ_s and κ_t are the hopping parameters in space and time direction and are related to the continuum parameters

$$g_0 = \frac{6\lambda}{\xi\kappa_s^2} \;\; ; \;\; \phi_0(x) = \frac{\sqrt{2\xi\kappa_s}}{a_s}\Phi(x) - v_0 \qquad (4)$$

$$m_0^2 = 2\frac{6\kappa_s + 2\xi^2\kappa_s - 1 + 2\lambda}{\kappa_s a_s^2} \;\; ; \;\; v_0^2 = \frac{\xi\kappa_s(6\kappa_s + 2\xi^2\kappa_s - 1 + 2\lambda)}{a_s^2\lambda} \qquad (5)$$

a_s and a_t are the lattice spacings in space and time direction and the anisotropy is defined through

$$\xi = \sqrt{\frac{\kappa_t}{\kappa_s}} \approx \frac{a_s}{a_t} \tag{6}$$

The last relation is only exact at tree level [14]. For $\lambda \to \infty$ and fixed κ_s, κ_t the theory reduces to the Ising model: $\Phi(x) = \pm 1$.

QFT at finite temperature T can be described by the imaginary time formalism ITF [15], which handles this problem in the Feynman's functional formalism by "Wick"rotating the time in the imaginary direction and imposing a period of $1/T$. Therefore, finite temperature on the lattice can be considered by a finite extension N_t in the time direction of the lattice with periodic boundary conditions. This corresponds to a temperature

$$T = \frac{1}{N_t a_t} \approx \frac{\xi}{N_t a_s} \tag{7}$$

By tuning ξ and N_t for fixed a_s one can change the temperature. But due to the lower limit of $N_t = 1$ the anisotropy often is necessary in order to reach a high enough temperature. A fixed physical temperature in the continuum means the correlated limit

$$a_s \to 0 \ , \ a_t \to 0 \ , \ N_t \to \infty \ ; \ N_t a_t \ fixed \tag{8}$$

3 The CCPs at finite temperature

How can symmetry restoration occur and be detected in a lattice regularized model? The problem is that for the physical interpretation one must suitably tune the bare parameters toward a phase transition. The central idea behind this procedure are "curves of constant physics (CCP)" [16]. In case of a ϕ^4 theory these curves are parametrized by the renormalized coupling g_R. The renormalized mass m_R serves as a "reference quantity". In order to obtain a continuum limit physical quantities must be constant along a CCP in the vicinity of the critical point up to corrections ("lattice artifacts") of order $a_{s,t}$. In the scaling region near a critical point the CCPs are independent of the choice of the reference quantity m_R (or equivalently the lattice parameter $a_{s,t}$).

In order to extract continuum physics, we must move along a CCP. As the lattice spacing $a_{s,t}$ changes along such a line, this implies a change in the temperature $T = 1/N_t a_t$. To control scaling a new dimensionless physical quantity T/m_R must be taken into account. Therefore, when approaching the second-order line, where the continuum limit is taken, one simultaneously has to change N_t in such a way that the physical temperature T/m_R is kept constant. By measuring suitable order parameters for symmetry breaking one can look for the scaling region, where the quantities do not change any more, and detect a possible symmetry restoration. The most interesting question is of course, at which temperature does the transition occur for a given value of g_R, and how well T_{sr}/m_R compares with the predictions of perturbation theory.

As moving along a CCP with constant g_R implies a change of the bare coupling λ, the exposed scheme cannot be fulfilled in the Ising limit. Scaling checks can only be done by varying λ. Therefore we simply alter the hopping parameter κ, so crossing the CCPs, determine the phase transition point for various time extensions and various lattices, and interpret our results by making scaling arguments and perturbative computations.

4 Perturbation theory at finite temperature

In this chapter a one-loop perturbative expansion up to order g_R of the renormalized coupling in the broken phase is presented in the continuum and on the lattice.

The renormalized quantities in the continuum at zero and non-zero temperature are defined with the help of the following Lagrangian according to Eq.(1) and Eq.(2)

$$-L = \frac{1}{2}(\partial_\mu \phi_R(x))(\partial^\mu \phi_R(x)) + \frac{1}{2} m_R^2 \phi_R(x)^2 + \frac{1}{6} g_R v_R \phi_R(x)^3 + \frac{1}{24} g_R \phi_R(x)^4 \tag{9}$$

with

$$v_R^2 = \frac{3 m_R^2}{g_R} \tag{10}$$

The lower R-index marks the renormalized quantities at zero temperature and the corresponding T-index at non-zero temperature.

The one-loop computation on the lattice is similar to Ref.[2], where the corrections to the renormalized quantities were derived on a finite volume. The results for the wave function renormalization Z_T, the renormalized mass m_T, the renormalized coupling g_T, and the renormalized expectation value of the wave function v_T are

$$Z_T = Z_R(1 - \frac{3}{2} g_R m_R^2 \delta I) \tag{11}$$

$$m_T^2 = m_R^2 - g_R \delta J_1 - \frac{3}{2} g_R m_R^2 \delta J_2 - \frac{3}{2} g_R m_R^4 \delta I \tag{12}$$

$$g_T = g_R - \frac{3}{2} g_R^2 \delta J_2 - 3 g_R^2 m_R^2 \delta I \tag{13}$$

$$v_T = v_R \left(1 - \frac{g_R}{2 m_R^2} \delta J_1 + \frac{3}{4} g_R m_R^2 \delta I\right) \tag{14}$$

The lattice integrals $J_n^L(N_s, N_t)$ are defined as

$$J_n^L(N_s, N_t) = \frac{\xi}{N_s^3 N_t} \sum_{\underline{k}, k_4} \left(\frac{1}{\xi^2 \hat{k}_4^{\ 2} + \hat{\underline{k}}^2 + m_R^2} \right)^n \tag{15}$$

with the conventions

$$\hat{k}_\mu = 2 \sin\left(\frac{1}{2} k_\mu\right) \ ; \ \mu = 1, ..., 4$$

$$k_i = \frac{2\pi}{N_s} l_i \ ; \ l_i = 0, ..., N_s - 1 \ ; \ i = 1, ..., 3$$

$$k_4 = \frac{2\pi}{N_t} l_4 \ ; \ l_4 = 0, ..., N_t - 1$$

and δJ_n^L is

$$\delta J_n^L = J_n^L(N_s, N_t) - J_n^L(\infty, \infty) \tag{16}$$

The corresponding integral $I^L(N_s, N_t)$, which results from the wave function renormalization, is

$$I^L(N_s, N_t) = \frac{\xi}{3 N_s^3 N_t} \sum_{\underline{k}, k_4} \left[\frac{\sum_i \cos k_i}{\left(\xi^2 \hat{k}_4^{\ 2} + \hat{\underline{k}}^2 + m_R^2\right)^3} - \frac{4 \sum_i \sin^2 k_i}{\left(\xi^2 \hat{k}_4^{\ 2} + \hat{\underline{k}}^2 + m_R^2\right)^4} \right] \tag{17}$$

In the limit

$$a_s \to 0 \; ; \; a_t \to 0 \; ; \; N_s \to \infty \tag{18}$$

the discrete summation in time direction can be done explicitly by an analytic continuation [17]. For example, the integral δJ_1^C has the well-known form

$$\delta J_1^C = \frac{1}{(2\pi)^3} \int_{-\infty}^{\infty} d^3\underline{k} \frac{1}{\exp\left(1/T\sqrt{\underline{k}^2 + m_R^2}\right) - 1} \frac{1}{\sqrt{\underline{k}^2 + m_R^2}} \tag{19}$$

The index C marks this continuum limit of the integrals, the index L the lattice form. No index as in Eq.(11-14) means any of them.

Note that, by taking the integral $I^L(N_s, N_t)$ of Eq.(17), the wave function renormalization is done in the space directions. There is a slight difference to the time direction, even in the limit of Eq.(18), since finite temperature explicitly disturbs Lorentz invariance.

At high temperatures $T/m_R \gg 1$ the dominant term in Eq.(12) is δJ_1. Using its asymptotic expansion one gets the well-known formula [5]

$$m_T^2 = m_R^2 - \frac{1}{12} g_R T^2 \tag{20}$$

The symmetry restoration sets in when the mass m_T disappears. Eq.(20) leads to

$$\frac{T_{sr}}{m_R} = \sqrt{\frac{12}{g_R}} \tag{21}$$

This result would have also been obtained when setting the propagating mass to zero in Eq.(12). But we will see from Eq.(24) that this procedure is outside the validity of the used approximations.

Inserting Eq.(21) into Eq.(14) one realizes that the vacuum expectation value is not zero at T_{sr} in the one-loop expansion. As the one-loop derivation is based on the assumption that the fluctuations around the vacuum expectation value are small, one has to improve the above formulas near the phase transition in order to get consistent results. Since the failure of the above method is due to the small propagating mass m_T which is quite different from the zeroth order mass m_R, it is necessary to use an improved mass for propagation which leads to the well-known "improved" loop expansion [5][6]. Instead of m_R^2, the better approximation

$$m_R^2 \to m_R^2 - g_R \delta J_1 \tag{22}$$

is taken in the propagators.

The validity of the improved expansion is limited by the requirement

$$g_R \delta J_2(m_T^2) \ll 1 \tag{23}$$

At high temperatures the allowed region for T can explicitly be given by using the asymptotic expansion of δJ_2

$$|T_{sr} - T| \gg \frac{g_R}{16\pi^2} T_{sr} \tag{24}$$

In other words, the improvement does not help for $T \approx T_{sr}$.

5 The algorithm and the order parameters

The algorithm for updating the spin configurations is not the usual Metropolis-algorithm, but a so-called percolation cluster algorithm [18][19]. In contrast to local spin flips of the Metropolis version it creates new spin configurations by flipping well defined clusters of spins. The advantages are twofold:

- Due to its non-local character this algorithm reduces the phenomenon of critical slowing down near the critical point [18].
- By measuring cluster variables one can achieve a variance reduction [19]. Instead of the original physical quantities one uses related ones with the same expectation value, but reduced fluctuations.

We have to measure the critical hopping parameter κ_c in order to get the symmetry restoration temperature. Here we are confronted with the problem of finding an order parameter M distinguishing the two different phases. It is well-known that there is no spontaneous symmetry breaking in a finite volume. The correct continuum limit for the magnitization is first the infinite volume limit and then the zero limit of the external field inhibiting a non-zero order parameter on a finite lattice. Nevertheless, there is a distribution function for the order parameter, which is doubly peaked [20]. The continual spin-updating enables a tunneling from one peak to the other averaging M to zero [2]. So we decide to distinguish one peak. A transition to the other peak is corrected by a corresponding symmetry transformation. The final result is that we measure $|M|$ instead of M. It is expected that this definition converges to the correct infinite volume limit for large volumes [20]. We also measure the quantity M_0, which is the magnitization of the largest cluster, in order to test our expectation that there is a single large background cluster and a large number of small clusters of random signs, even near the critical point, and so the shifting of κ_c due to finite size effects is small. The susceptibility χ is determined, too, to get a more reliable estimation of κ_c. As an example, the cluster observable of χ is presented

$$\chi = \frac{1}{N_s^3 N_t} \left[\left\langle \sum_{x,y} s_x s_y \delta_{xy} \right\rangle - \left\langle \left| \sum_x s_x \right| \right\rangle^2 \right] \tag{25}$$

δ_{xy} is only non-zero if the spins s_x and s_y are in the same cluster. $< \ldots >$ means the ensemble average.

Having κ_c we must make use of the renormalized mass m_R at κ_c to get T_{sr}/m_R. The zero-temperature quantity m_R is derived as in [3]. But instead of using an hopping parameter expansion in the symmetric phase for an initial condition of the Callan-Symanzik equations, we take the initial value from a very precise Monte Carlo simulation directly in the broken phase. In Ref.[2] the quantities $m_R = 0.395$; $g_R = 30.6$; $Z_R = 0.918$ were measured at $\kappa_c = 0.076$. These values can serve as a starting point for the integration of the Callan-Symanzik functions, where three-loop β-functions and m_R^2-corrections in one-loop are taken into account.

6 Scaling analysis

Because of the simulations in the Ising limit we cannot move along a CCP and, therefore, are not able to test explicitly scaling violation, i.e. the presence of lattice artifacts. Therefore, we have to make scaling arguments in order to get an idea of the correctness of our results.

Let us make a naive analysis with the parameters ξ, N_s, N_t. In order to reach the continuum limit being exposed in Eq.(8) we demand

- $1/(N_s a_s) \ll 1/a_s \Rightarrow N_s \gg 1$ for avoiding lattice effects in space direction.
- $1/(N_t a_t) \ll 1/a_s \Rightarrow N_t \gg \xi$ for avoiding lattice effects in time direction.
- $1/(N_s a_s) \ll 1/(N_t a_t) \Rightarrow \xi N_s \gg N_t$ for getting the correlated continuum limit.

This crude estimation is in agreement with [21], where the energy density of a non-interacting Bose system has been analytically computed and compared with the continuum theory.

$N_s \gg N_t$ can be confirmed by investigating the critical coefficients of the susceptibility and of the order parameters. The values of a three-dimensional instead of a four-dimensional Ising system must be obtained, i.e.

$$\nu_3 = 0.64 \; ; \; \gamma_3 = 1.25 \; ; \; \beta_3 = 0.31 \tag{26}$$

instead of

$$\nu_4 = 0.5 \; ; \; \gamma_4 = 1.0 \; ; \; \beta_4 = 0.5 \tag{27}$$

$N_s \gg 1$ can explicitly and non-perturbatively be tested by finite size scaling FSS [22]. For the order parameter M (either $|M|$ or M_0) we choose the usual way by searching for an unique scaling function f with

$$M N_s^{\beta/\nu} = f\left(t N_s^{1/\nu}\right) \; ; \; t = (\kappa - \kappa_c)/\kappa_c \tag{28}$$

FSS is an additional test for the correctness of the critical coefficients. In order to incorporate the small shifting of the critical hopping parameter we make an explicit ansatz for the susceptibility [23]

$$\chi = A_1 \left\{ N_s^{-\alpha_0/\nu} + A_{2,3} |\kappa - \kappa_c)|^{\alpha_0} \right\}^{-\gamma/\alpha_0} \tag{29}$$

$A_1, A_{2,3}$ are fitted parameters and α_0 is at will. $A_{2,3}$ means a constant A_2 for $(\kappa - \kappa_c) < 0$ and a constant A_3 for $(\kappa - \kappa_c) > 0$. The formula Eq.(29) incorporates two limits of FSS

$$\chi = A_1 N_s^{\gamma/\nu} \; ; \; |\kappa - \kappa_c| \ll 1 \tag{30}$$

and

$$\chi = A_1 A_{2,3} |\kappa - \kappa_c|^{-\gamma} \; ; \; |\kappa - \kappa_c| \gg 1 \tag{31}$$

We take $\alpha_0 = 2$, as this value already gives reliable results.

The requirement $N_t \gg 1$ is problematic. There is no scaling function to test for scaling due to the cross-over of the sytem from a three-dimensional Ising model to a four-dimensional one, mixing the critical coefficients at will. We try to make comparison with the values T_{sr}/m_R of the perturbation theory in order to get information about lattice artifacts in our measurements due to finite N_t. According to Eq.(21) we expect good agreement for high temperatures, since the mass m_R being responsible for lattice corrections has disappeared.

7 Results

The simulations were performed on various lattices in order to get reliable information about the symmetry restoration, namely $12^3 \times 3, 12^3 \times 4, 12^3 \times 6, 12^3 \times 12, 16^3 \times 4, 20^3 \times 4, 20^3 \times 5$. Simulations were done on isotropic and anisotropic lattices, but due to the lack of precise values of the renormalized mass m_R for anisotropic parameters only data measured with $\xi = 1$ are presented. The number of sweeps per value of κ was 100000 with 4000 configurations at the beginning being used for thermalization.

We did not use lattices with a time extension N_t smaller than three, because we realized that the critical point is outside the scaling region $m_R < 0.5$ and, therefore, surely plagued by lattice artifacts. We did not use lattices with a space extension N_s smaller than twelve in order to avoid highly non-perturbative tunneling effects, which are relevant for lattices of smaller sizes [2].

The first measurements were performed on $12^3 \times 4, 16^3 \times 4, 20^3 \times 4$ lattices. Fig.1 shows the two order parameters $|M|$(filled circle) and M_0(square) for a $16^3 \times 4$ lattice. As the error bars are within the symbols, they are not presented (this holds for all the figures, where error bars are missing). One sees good agreement of the two order parameters in the broken phase and at the critical point. The full line is a crude fit of the form

$$|M| \sim t^{\beta_3} = t^{0.31} \; ; \; t = \frac{\kappa - \kappa_c}{\kappa_c} \tag{32}$$

This curve is of clearly better agreement than the dashed line, which is a fit with four-dimensional parameters

$$|M| \sim t^{\beta_4} (\ln t)^{1/3} = t^{1/2} (\ln t)^{1/3} \tag{33}$$

In order to verify the critical coefficients we search explicitly for the scaling function according to Eq.(28). Fig.2 is definitely in better agreement than Fig.3 so fulfilling the requirement $N_s \gg N_t$.

Next we try to determine the critical hopping parameter with the help of the susceptibility χ , as defined in Eq.(25). In Fig.4 the susceptibilities of a $20^3 \times 4$(diamond), a $16^3 \times 4$(circle), and a $12^3 \times 4$ (square) lattice are shown. The additional full line is the scaling ansatz Eq.(29) with three-dimensional coefficients and the dashed line with four-dimensional ones. Due to the similar factors γ_3/ν_3=1.95 and γ_4/ν_4=2.0 the differences are not so pregnant as for the order parameters. We see a small shifting of κ_c from about 0.07595 for $20^3 \times 4$ to 0.07605 for $12^3 \times 4$, but the movement is too vague in order to make a reliable extrapolation to infinite length. $N_s \gg N_t$ is approximately valid even for a $12^3 \times 4$ lattice. Let us repeat the result:

$$\kappa_c = 0.0760(1) \; ; \; 16^3 \times 4 \; \textit{lattice}$$

The next simulations were performed on lattices $12^3 \times 3$ and $20^3 \times 5$. Again the susceptibility is used for the determination of κ_c. We get

$$\kappa_c = 0.0755(1) \; ; \; 20^3 \times 5 \; \textit{lattice}$$

and

$$\kappa_c = 0.0771(1) \; ; \; 12^3 \times 3 \; \textit{lattice}$$

The values of the renormalized masses m_R at the corresponding critical points are used to determine T_{sr}/m_R. Fig.5 shows T_{sr}/m_R as a function of the renormalized coupling g_R.

The circles are the results for $N_t = 3, 4, 5$. Using the extrapolated m_R from Ref.[3] the points are shifted slightly downwards. The dashed line is the behaviour of T_{sr}/m_R in the high-temperature limit Eq.(21). The two dashed-dotted lines are the upper and lower bounds of T_{sr}/m_R according to Eq.(24). The errors were roughly estimated by assuming a change of 5% in the mass m_R when varying κ in the last digit by one. One surprisingly realizes that the high-temperature limit is in very good agreement with the measured points in spite of the fact that $T_{sr}/m_R < 1$. In order to estimate the results correctly we also have to compare with the exact continuum and lattice results in one-loop. The full lines in Fig.6 are the results for T_{sr}/m_R, which are got from setting m_T to zero in Eq.(12). C means the continuum and L the lattice approximation. The dashed-dotted lines are the corresponding solutions for the optimized expansion. Although the differences to our measured values are small, especially for the optimized expansion, there is a significant deviation which is a sign for the importance of higher loops. This will be clear from Fig.7. Now T_{sr}/m_R is shown as a function of N_s for constant $N_t = 4$. The notation is identical to Fig.6. The one-loop lattice results predict a much larger variation of κ_c than was measured in the simulations. One must remind that these lattices have a totally three-dimensional behaviour and, therefore, our simple mean-field like computation, which starts from a four-dimensional zero-temperature theory, is probably not able to take into account the strong non-perturbative effects that are related with such a transition. This becomes more apparent from Fig.8. Now we consider T_{sr}/m_R is a function of N_t for constant $N_s = 12$. The circles are the measurements on $12^3 \times 4$, $12^3 \times 6$, and $12^3 \times 12$ lattices. The $12^3 \times 3$ lattice is not considered as its m_R value lies outside the scaling region and so we cannot use the Callan-Symanzik functions in order to determine m_R. But as we know that its point is lying on the dashed line, we realize that the perturbation theory does not describe the point correctly. Now the explanation is clear. As long as the full line does not cross the dashed line, perturbation theory does describe the value of T_{sr}/m_R correctly being a hint for the four-dimensional behaviour of the lattice. The cross-over between the four- and the three-dimensional theory is lying somewhere around the intersection point. By determinating this intersection point for different lattices $N_s^3 \times N_t$ one can estimate a lower bound for N_s/N_t in order that a reliable estimation of T_{sr}/m_R is possible.

$$\frac{N_s}{N_t} > 3 \tag{34}$$

Of course, this is a very crude estimation from perturbation theory as we do not know the exact behaviour of the curve near the intersection point. There is probably a smoothening implying lower values of N_t and, therefore, a greater value in Eq.(34).

Note that our above analysis is based on the assumption that Eq.(21) is almost correct even for small temperatures in contrast to the simple perturbation theory. This implies that the agreement between this relation and our measured points is not caused by non-perturbative lattice effects but corresponds to the continuum theory. As perturbation theory is getting more reliable when approaching the critical line, we can assume that Eq.(21) is valid in the whole scaling region.

8 Summary

We made numerous simulations on various lattices in order to get an idea of symmetry restoration on the lattice and its relation with the continuum theory. In the framework of

perturbation theory we got good agreement with the measurements and were able to explain the appearing differences. We concluded that the relation

$$\frac{T_{sr}}{m_R} \approx \sqrt{\frac{12}{g_R}}$$

is probably valid in the whole scaling region of the Ising model and, therefore, in the scaling region of the ϕ^4 theory for all values of the self-coupling λ, since the extreme Ising limit would be very sensitive for deviations.

When taking the expectation value of the Higgs sector and assuming the influence of the gauge coupling to be small this implies for the symmetry restoration

$$T_{sr} = 2v_R \approx 500\ GeV$$

From our data we conclude that $T_{sr}/m_R > 0.6$ in the scaling region and, therefore,

$$m_R < \frac{T_{sr}}{0.6} \approx 830\ GeV$$

This can be taken as a crude upper bound for the Higgs mass, based on a single component Φ^4 theory.

References

[1] I. Montvay, Phys. Lett. **172B** (1986) 71; Nucl. Phys. **B293** (1987) 479

[2] K. Jansen, J. Jersak, I. Montvay, G. Münster, T. Trappenberg, U. Wolff, Phys. Lett. **213B** (1988) 203;
K. Jansen, I. Montvay, G. Münster, T. Trappenberg, U. Wolff, DESY preprint 88-169 (1988), to appear in Nucl. Phys. B

[3] M. Lüscher, P. Weisz, Nucl. Phys. **B290 [FS20]** (1987) 25; Nucl. Phys. **B295 [FS21]** (1988) 65

[4] D. A. Kirzhniz, A. D. Linde, Phys. Lett. **42B** (1972) 471; JETP **40** (1974) 628

[5] S. Weinberg, Phys. Rev. **D9** (1974) 3357;
L. Dolan, R. Jackiw, Phys. Rev. **D9** (1974) 3320

[6] P. Fendley, Phys. Lett. **B196** (1987) 175

[7] A. Okopinska, Phys. Rev. **D35** (1987) 1835; Phys. Rev. **D36** (1987) 2415

[8] R. N. Mohapatra, G. Senjanović, Phys. Rev. **D20** (1979) 3390;
E. Manesis, S. Sakakibara, Phys. Lett. **157B** (1985) 287

[9] J. Iliopoulos, C. Itzykson, A. Martin, Rev. Mod. Phys. **47** (1975) 165

[10] M. G. do Amaral, C. A. Aragao de Carvalho, M. E. Pol, R. C. Shellard, Phys. Lett. **165B** (1985) 117; Z. Phys. **C32** (1986) 609

[11] L. von Lõhneysen, I. O. Stamatescu, R. E. Shrock, Phys. Lett. **B205** (1988) 321

[12] R. H. Brandenberger, Rev. Mod. Phys. **57** (1985) 1

[13] H. Kühnelt, C. B. Lang, G. Vones, Nucl. Phys. **B230 [FS10]** (1984) 16

[14] F. Karsch, Nucl. Phys. **B205 [FS5]** (1982) 285;
G. Burgers, F. Karsch, A. Nakamura, I. O. Stamatescu, Nucl. Phys. **B304** (1988) 587

[15] N. P. Landsman, Ch. G. van Weert, Phys. Rep. **145** (1987) 142

[16] I. Montvay, Nucl. Phys. **B269** (1986) 170;
W. Langguth, I. Montvay, P. Weisz, Nucl. Phys. **B277** (1986) 11

[17] M. B. Kislinger, P. D. Morley, Phys. Rev. **D13** (1976) 2771; Phys. Rep. **51** (1979) 63

[18] R. H. Swendson, J. S. Wang, Phys. Rev. Lett. **58** (1987) 86

[19] U. Wolff, Phys. Rev. Lett. **60** (1988) 1461; Nucl. Phys. **B300 [FS22]** (1988) 501

[20] K. Binder, Z. Phys. **B43** (1981) 119

[21] J. Engels, F. Karsch, H. Satz, Nucl. Phys. **B205 [FS5]** (1982) 239

[22] M. N. Barber, in *Phase transitions and critical phenomena* , eds. C. Domb, J. Lebowitz (Academic Press, New York, 1984) vol.8, p.146

[23] M. Tomiya, T. Hattori, Phys. Lett. **140B** (1984) 370

Figure captions

Fig. 1 The order parameters $|M|$ (filled circle) and M_0 (square) for a $16^3 \times 4$ lattice as a function of the hopping parameter κ. The full line is a fit according to Eq.(32), the dashed line is a fit according to Eq.(33) and $\kappa_c \approx 0.076$ is assumed.

Fig. 2 The scaling function from Eq.(28) with three-dimensional critical coefficients for the lattices $12^3 \times 4$ (square), $16^3 \times 4$ (circle), and $20^3 \times 4$ (diamond). The scaling length L is N_s.

Fig. 3 The scaling function from Eq.(28) with four-dimensional critical coefficients for the lattices $12^3 \times 4$ (square), $16^3 \times 4$ (circle), and $20^3 \times 4$ (diamond). The scaling length L is N_s.

Fig. 4 The susceptibility χ for the lattices $12^3 \times 4$ (square), $16^3 \times 4$ (circle), and $20^3 \times 4$ (diamond) as a function of the hopping parameter κ. The full line is a fit according Eq.(29) with three-dimensional critical coefficients, and the dashed line is a fit with four-dimensional coefficients. The critical hopping parameter $\kappa_c = 0.076$ is used.

Fig. 5 The symmetry restoration T_{sr}/m_R as a function of the renormalized coupling g_R. The three circles are the measured values on $12^3 \times 3$, $16^3 \times 4$, and $20^3 \times 5$ lattices. The dashed line is the value from Eq.(21). The two dashed-dotted lines are lower and upper bounds from Eq.(24).

Fig. 6 The one-loop approximation for T_{sr}/m_R from $m_T = 0$ in Eq.(12) as a function of N_t. The full line with C means in the continuum and the full line with L on the lattice. For the considered lattices $N_s/N_t = 4$ is constant. The dashed-dotted lines are the corresponding optimized expansions. The dashed line is T_{sr}/m_R from Eq.(21).

Fig. 7 The one-loop approximation for T_{sr}/m_R as a function of N_s and for constant $N_t = 4$. The full line with L is the approximation for the lattice and the full line with C in the continuum. The dashed-dotted lines are the corresponding optimized expansions. The dashed line is T_{sr}/m_R from Eq.(21). The circles are the measured values on $12^3 \times 4$, $16^3 \times 4$, and $20^3 \times 4$ lattices.

Fig. 8 T_{sr}/m_R as a function of N_t and for constant $N_s = 12$. The full line with L is the one-loop approximation for the lattice and the full line with C in the continuum. The dashed-dotted line is the optimized expansion for the lattice. The dashed line is the value from Eq.(21). The circles are the measured symmetry restoration temperatures on $12^3 \times 4$, $12^3 \times 6$, and $12^3 \times 12$ lattices.

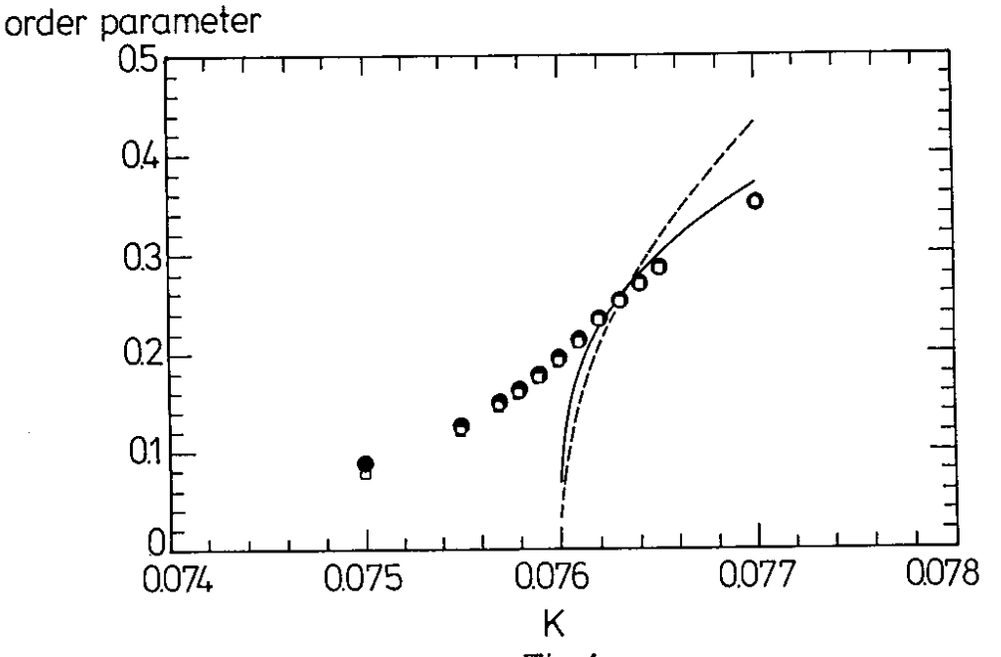

Fig.1

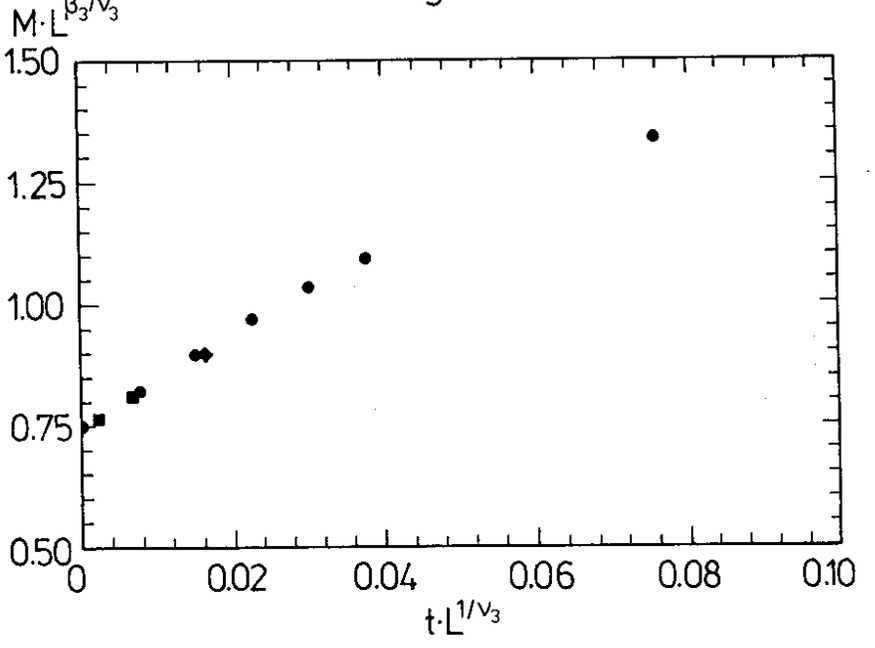

Fig.2

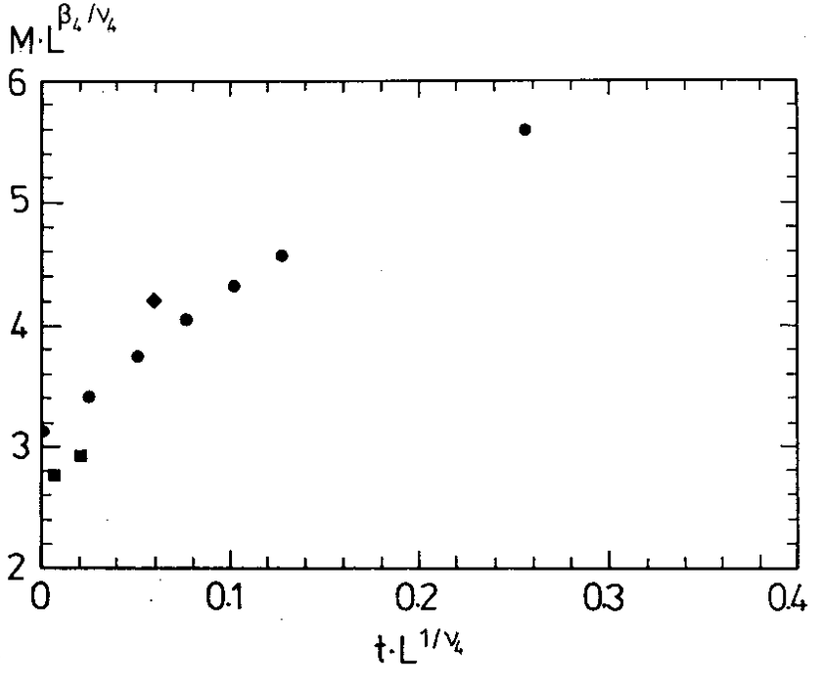
M·L^{β4/ν4}
6
5
4
3
2
0
0.1
0.2
0.3
0.4
t·L^{1/ν4}

Fig. 3

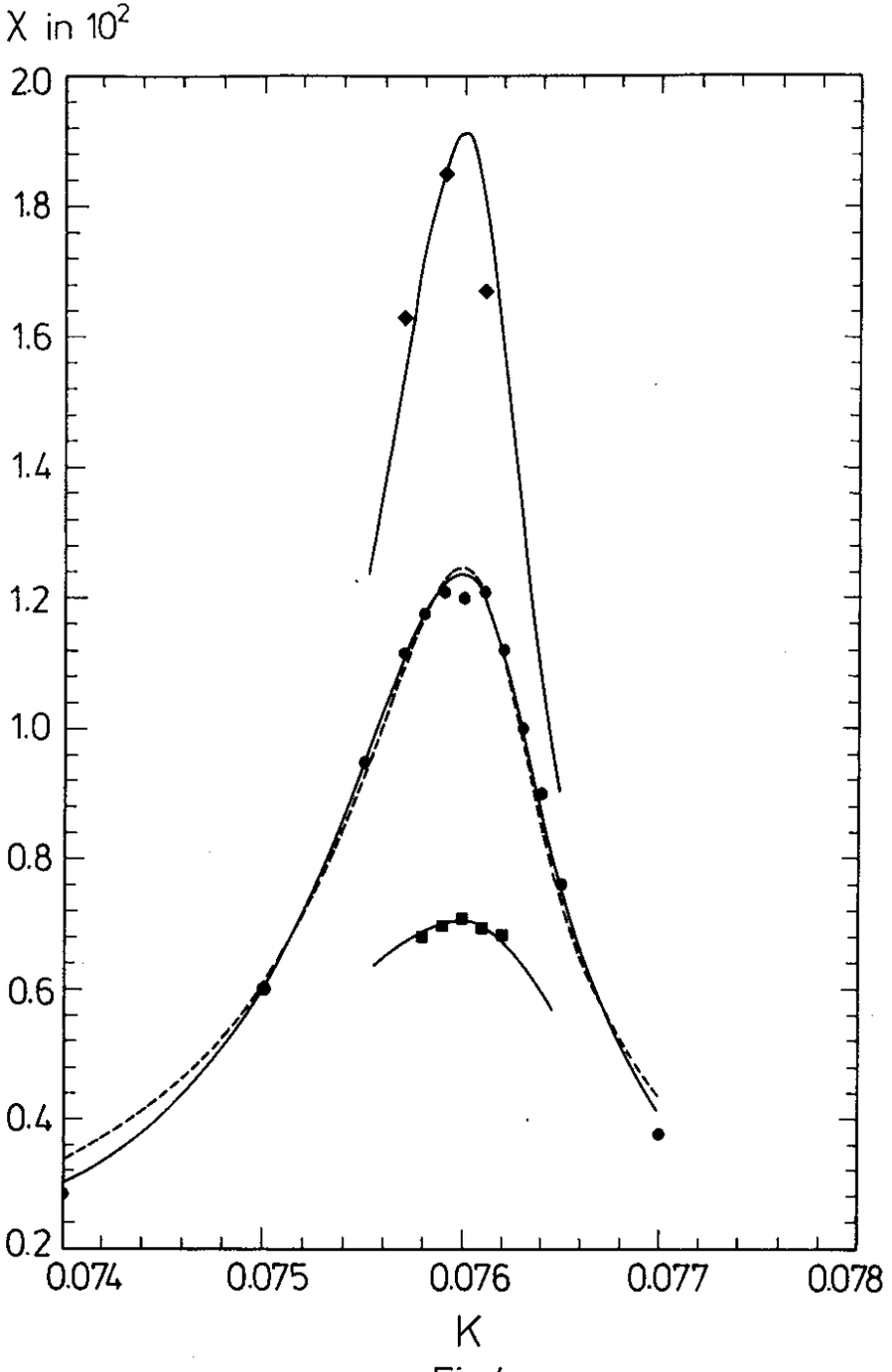
X in 10²
2.0
1.8
1.6
1.4
1.2
1.0
0.8
0.6
0.4
0.2
0.074
0.075
0.076
0.077
0.078
K

Fig. 4

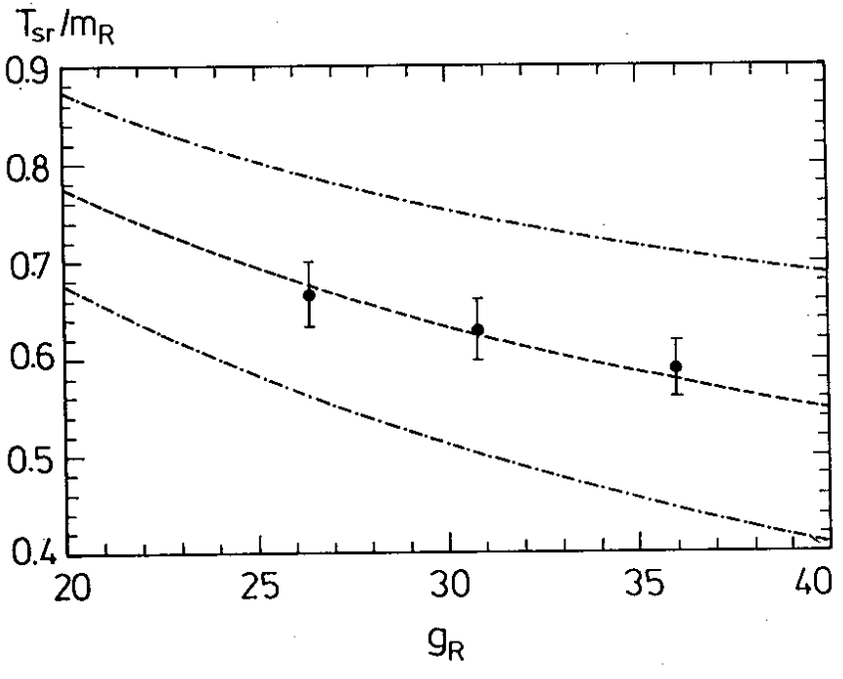
T_{sr}/m_R
0.9
0.8
0.7
0.6
0.5
0.4
20
25
30
35
40
g_R

Fig. 5

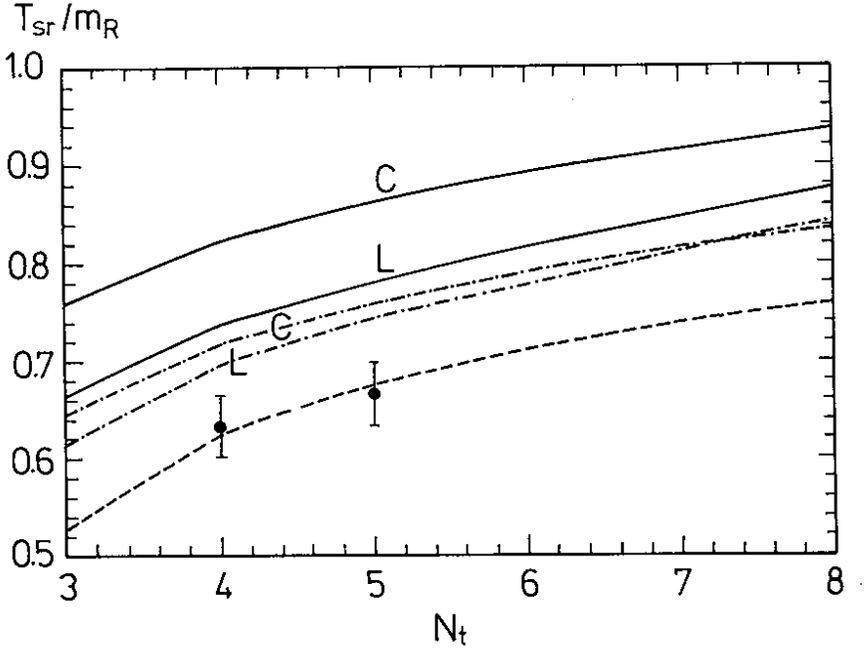
T_{sr}/m_R
1.0
0.9
0.8
0.7
0.6
0.5
C
L
C
L
3
4
5
6
7
8
N_t

Fig. 6

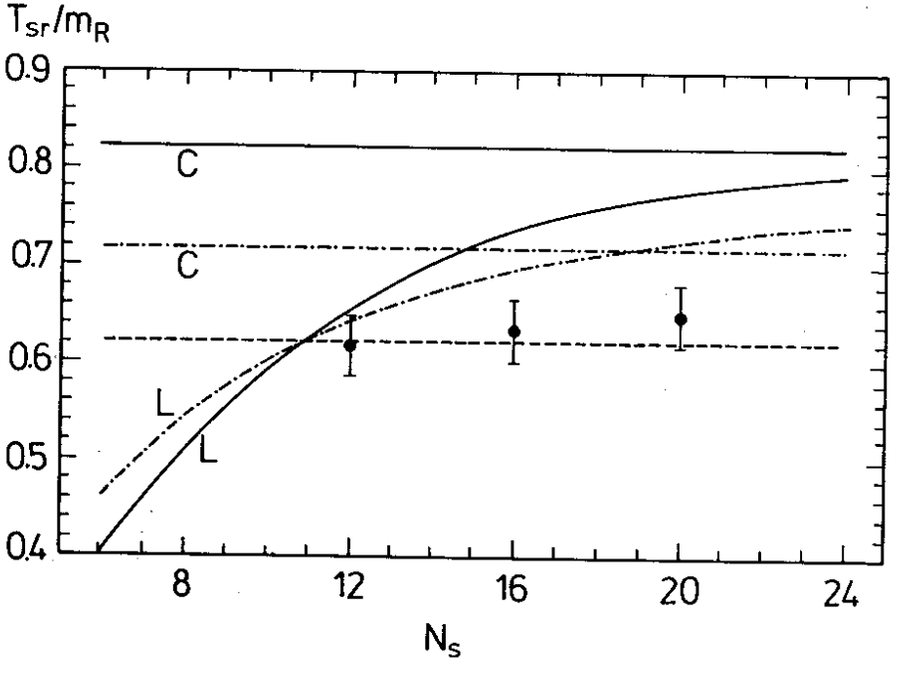
T_{sr}/m_R
0.9
0.8
0.7
0.6
0.5
0.4
C
C
L
L
8
12
16
20
24
N_s

Fig.7

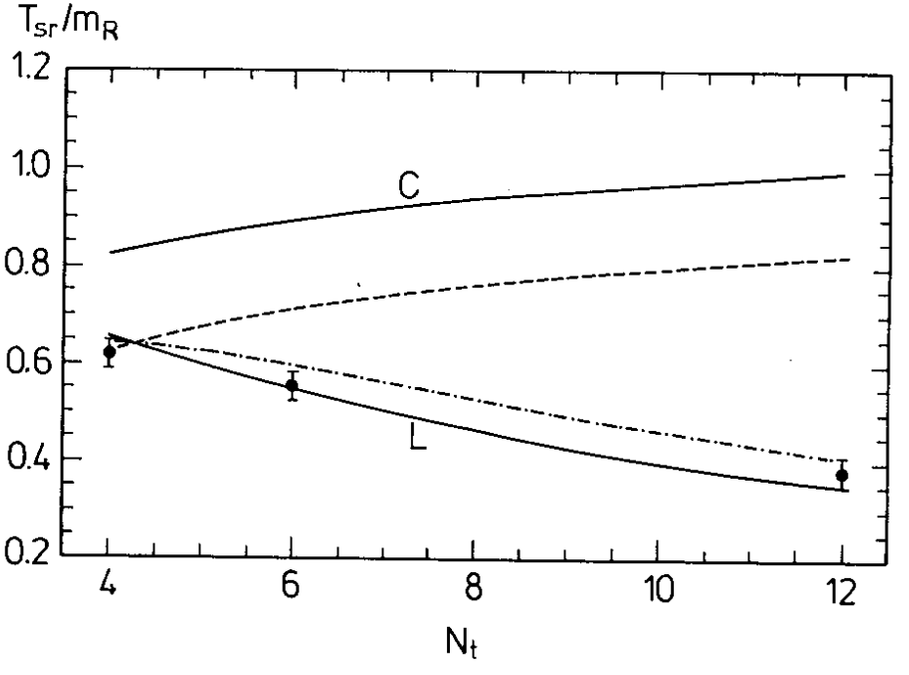
T_{sr}/m_R
1.2
1.0
0.8
0.6
0.4
0.2
C
L
4
6
8
10
12
N_t

Fig.8